Supporting information

Pyrazine Dicarboxylate-Bridged Arsenotungstate : Synthesis, Characterization, and Catalytic Activities in Epoxidation of Olefins and Oxidation of Alcohols

Xinyi Ma, Peipei He, Baijie Xu, Jingkun Lu, Rong Wan, Hechen Wu, Yuan Wan, Pengtao Ma, Jingyang Niu* and Jingping Wang*

Henan Key Laboratory of Polyoxometalate Chemistry, Institute of Molecular and Crystal Engineering, College of Chemistry and Chemical Engineering, Henan University, Kaifeng, Henan 475004 P.R. China

E-mail address: jyniu@henu.edu.cn, jpwang@henu.edu.cn
Fax: (+86)371-23886876

CONTENTS

Section1. Summary of the previously reported typical of ATs

Table S1. Summary of the reported ATs based on different carboxylate ligands

Group	Formula	Precursor	Year	Ref
Wang's group	$[Ce_4As_4W_{44}O_{151}(ala)_4(OH)_2(H_2O)_{10}]^{12-}$ (ala = alanine)	$Na_9[B\text{-}\alpha\text{-}AsW_9O_{33}]$	2007	1
Xu's group	$[Dy_2(Hcit)_2(AsW_{10}O_{38})]^{11-}$ (Hcit = citric acid)	$Na_9[B\text{-}\alpha\text{-}AsW_9O_{33}]$	2012	2
Li's group	$[RE_6(H_2O)x\{As_4W_{44}(OH)_2(proline)_2O_{151}\}]^{10-}$ (RE = Tb^{III}, Dy^{III}, x = 22; RE = Nd^{III}, x = 26)	$K_{14}[As_2W_{19}O_{67}(H_2O)]$	2013	3
Boskovic's group	$[Gd_6As_6W_{65}O_{229}(OH)_4(H_2O)(OAc)_2]^{38-}$ $[Yb_{10}As_{10}W_{88}O_{308}(OH)_8(H_2O)_{28}(OAc)_4]^{40-}$	$K_{14}[As_2W_{19}O_{67}(H_2O)]$	2009	4
	$[Dy_4As_2W_{22}O_{76}(H_2O)_{19}(C_2H_5NO_2)_2]^{2-}$ ($C_2H_5NO_2$ = glycine)	$K_{14}[As_2W_{19}O_{67}(H_2O)]$	2010	5
	$\{Tb_2(pic)(H_2O)_2(B\text{-}\beta\text{-}AsW_8O_{30})_2[WO_2(pic)]_3\}^{10-}$ $\{Tb_8(pic)_6(H_2O)_{22}(B\text{-}\beta\text{-}AsW_8O_{30})_4[WO_2(pic)]_6\}^{12-}$ (pic = 2-picolinate)	$K_{14}[As_2W_{19}O_{67}(H_2O)]$	2010	6
	$[RE_4As_5W_{40}O_{144}(H_2O)_{10}(gly)_2]^{21-}$ (RE = Gd^{III}, Tb^{III}, Dy^{III}, Ho^{III}, Y^{III}) (gly = glycine)	$K_{14}[As_2W_{19}O_{67}(H_2O)]$	2011	7
	$[K_2\{Dy(H_2O)_3\}_2\{As_2W_{19}O_{68}\}\{WO_2(pic)\}_2]^{6-}$	$K_{14}[As_2W_{19}O_{67}(H_2O)]$	2011	8
	$[Eu_8(pic)_6(H_2O)_{22}(B\text{-}\beta\text{-}AsW_8O_{30})_4(WO_2(pic))_6]^{12-}$ (pic = 2-picolinate)	$K_{14}[As_2W_{19}O_{67}(H_2O)]$	2012	9
	$[As^{III}_4(Y^{III}W^{VI}_3)W^{VI}_{44}Y^{III}_4O_{159}(Gly)_8(H_2O)_{14}]^{9-}$ (gly = glycine)	$K_{14}[As_2W_{19}O_{67}(H_2O)]$	2014	10
Zhao's group	$[RE_2W_4O_{10}(H_2O)_8(Ser)_2(B\text{-}a\text{-}AsW_9O_{33})_2]^{8-}$ (RE^{3+} =Eu^{3+}, Gd^{3+}, Tb^{3+}, Dy^{3+}, Ho^{3+}, Er^{3+}, Tm^{3+}, Yb^{3+}, and Y^{3+}) (Ser = serine)	As_2O_3	2017	11
	$[RE(H_2O)_8]_2[Fe_4(H_2O)_8(L\text{-}thr)_2(B\text{-}\beta\text{-}AsW_9O_{33})_2]$ (RE = La^{III}, Pr^{III}, Nd^{III}, Sm^{III}, Eu^{III}, Gd^{III} ,Tb^{III}, Dy^{III}, Er^{III}) (L-thr = L-threonine)	$K_{14}[As_2W_{19}O_{67}(H_2O)]$	2015	12
Our group	$[As_6W_{58}O_{206}Ce_4(pydc)(H_2O)_6]^{38-}$ (pydc = pyridine-2,3-dicarboxylic acid)	$K_{14}[As_2W_{19}O_{67}(H_2O)]$	2014	13
	$[RE_2(C_4H_4O_6)(C_4H_2O_6)(AsW_9O_{33})]_2^{18-}$ (RE = Ho^{III}, Er^{III}, Tm^{III}, Yb^{III}, Lu^{III}, Y^{III}) ($C_4H_4O_6$ = tartrate)	$K_{14}[As_2W_{19}O_{67}(H_2O)]$	2015	14
	$\{RE_3(H_2O)_7[RE_2(H_2O)_4As_2W_{19}O_{68}(WO_2)_2(C_6O_7H_4)_2]_3\}^{33-}$ (RE=Y^{III}, Tb^{III}, Dy^{III}, Ho^{III}, Er^{III}, Tm^{III}, Yb^{III}, Lu^{III}) ($C_6H_8O_7$ = citric acid)	$K_{14}[As_2W_{19}O_{67}(H_2O)]$	2015	15

	$\{[RE_3(\mu_3\text{-}OH)(H_2O)_8(AsW_9O_{33})(AsW_{10}O_{35}(mal))]_2\}^{22-}$ (RE = Dy^{III}, Tb^{III}, Gd^{III}, Eu^{III}, Sm^{III}) (mal = malate)	$K_{14}[As_2W_{19}O_{67}(H_2O)]$	2015	16
	$[\{Pr(H_2O)_2\}_2\{As_2W_{19}O_{68}\}\{WO_2(mal)\}_2]^{12-}$	$K_{14}[As_2W_{19}O_{67}(H_2O)]$	2018	17
	$[Ce_4(H_2O)_{14}(pzdc)(H_2pzdc)As_3W_{29}O_{103}]^{13-}$ (pzdc = pyrizine-2,3-dicarboxylic acid)	$K_{14}[As_2W_{19}O_{67}(H_2O)]$	2018	18

[1] W. L. Chen, Y. G. Li, Y. H. Wang, E. B. Wang, Z. M. Su, *Dalton Trans.*, 2007, 4293–4301.

[2] F.Y. Li, W. H. Guo, L. Xu, L.F. Ma and Y.C. Wang, *Dalton Trans.*, 2012, **41**, 9220–9226.

[3] X.J. Feng, H.Y. Han, Y.H. Wang, L.L. Li, Y.G. Li and E.B. Wang, *CrystEngComm*, 2013, **15**, 7267–7273.

[4] F. Hussain, R. W. Gable, M. Speldrich, P. Kögerler and C. Boskovic, *Chem. Commun.*, 2009, 328–330.

[5] C. Ritchie, C. Boskovic, *Cryst. Growth Des*, 2010, **10**, 488-491.

[6] C. Ritchie, E. G. Moore, M. Speldrich, P. Kögerler and C. Boskovic, *Angew. Chem., Int. Ed.,* 2010, **49**, 7702–7705.

[7] C. Ritchie, M. Speldrich, R. W. Gable, L. Sorace, P. Kögerler and C. Boskovic, *Inorg. Chem.,* 2011, **50**, 7004–7014.

[8] C. Ritchie, C. E. Miller and C. Boskovic, *Dalton Trans.*, 2011, **40**, 12037–12039.

[9] C. Ritchie, V. Baslon, E. G. Moore, C. Reber and C. Boskovic, *Inorg. Chem.,* 2012, **51**, 1142–1151.

[10] M. Vonci, F. Akhlaghi Bagherjeri, P. D. Hall, R. W. Gable, A. Zavras, R. A. J. O'Hair, Y. Liu, J. Zhang, M. R. Field, M. B. Taylor, J. Du Plessis, G. Bryant, M. Riley, L. Sorace, P. A. Aparicio, X. López, J. M. Poblet, C. Ritchie and C. Boskovic, *Chem. – Eur. J.*, 2014, **20**, 14102–14111.

[11] H.L. Li, Y.J. Liu, J.L. Liu, L.J. Chen, J.W. Zhao and G.Y. Yang, *Chem. – Eur. J.,* 2017, **23**, 2673–2689.

[12] L.J. Chen, F. Zhang, X. Ma, J. Luo and J. W. Zhao, *Dalton Trans.*, 2015, **44**, 12598–12612.

[13] S. Z. Li, Y. Wang, P.T. Ma, J.P. Wang and J.Y. Niu, *CrystEngComm*, 2014, **16**, 10746–10749.

[14] Y. Wang, X.P. Sun, S.Z. Li, P.T. Ma, J.P. Wang and J.Y. Niu, *Dalton Trans.*, 2015, **44**, 733–738.

[15] Y. Wang, X.P. Sun, S.Z. Li, P.T. Ma, J.Y. Niu and J.P. Wang, *Cryst. Growth Des*, 2015, **15**, 2057–2063.

[16] P.T. Ma, R. Wan, Y.N. Si, F. Hu, Y.Y. Wang, J.Y. Niu and J.P. Wang, *Dalton Trans.*, 2015, **44**, 11514–11523.

[17] H.C. Wu, R. Wan, Y.N. Si, P.T. Ma, J.P. Wang, and J.Y. Niu, *Dalton Trans.*, 2018, **47**, 1958–1965.

[18] Y.J. Niu, Q.F. Xu, Y. Wang, Z. Li, J.K. Lu, P.T. Ma, C. Zhang, J.Y. Niu and J.P. Wang, *Dalton Trans.*, 2018, **47**, 9677–9684.

Section2. Additional structural figures

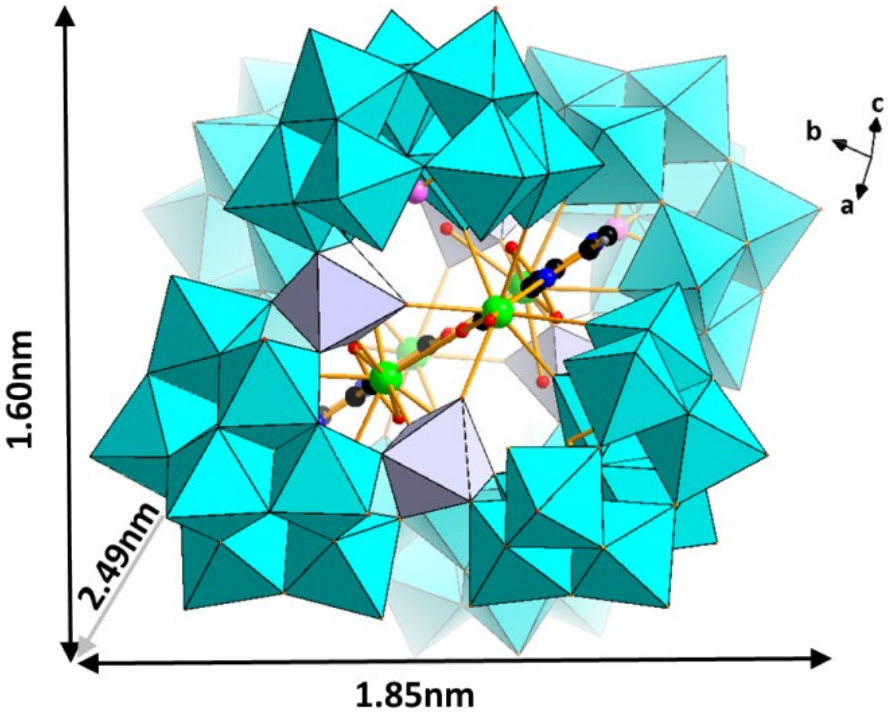

Fig. S1 Combination polyhedral/ball-and-stick representation of staggered pattern of the $[Pr_4(H_2O)_6(pzdc)_2As_6W_{58}O_{206}]^{38-}$ in **1**. Color code: WO_6, blue octahedra; As, pink; Pr, bright green; C, black; N, deep blue; O, red.

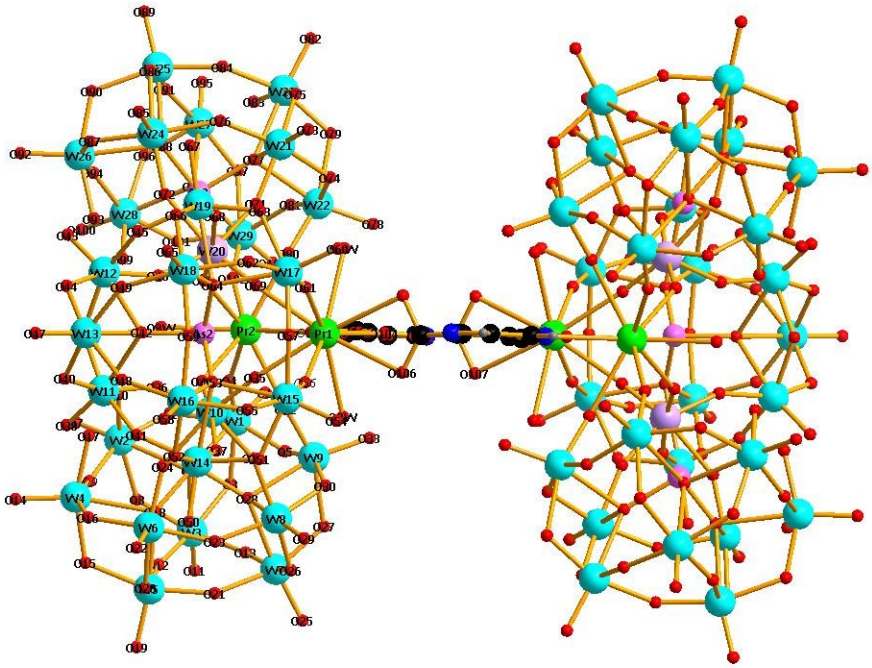

Fig. S2 The representation of W, Pr, As atoms and O atoms labeling in polyanion **1a**.

Section3. The BVS calculation results for W, Pr, As and O atoms in 1a

TableS2. The BVS calculation results for W, Pr, As and O atoms in 1a

Atom	BVS	Atom	BVS	Atom	BVS
Pr1	∑(Pr1)= 2.86	W8	∑(W8)=6.23	W19	∑(W19)=5.89
Pr2	∑(Pr2)= 3.01	W9	∑(W9)=6.15	W20	∑(W20)=6.16
As1	∑(As1)=3.00	W10	∑(W10)=6.02	W21	∑(W21)=6.32
As2	∑(As2)=2.97	W11	∑(W11)=5.76	W22	∑(W22)=6.21
As3	∑(As3)=3.49	W12	∑(W12)=5.75	W23	∑(W23)=6.28
W1	∑(W1)=5.99	W13	∑(W13)=6.01	W24	∑(W24)=6.25
W2	∑(W2)=6.13	W14	∑(W14)=6.30	W25	∑(W25)=6.01
W3	∑(W3)=6.32	W15	∑(W15)=6.33	W26	∑(W26)=5.78
W4	∑(W4)=5.41	W16	∑(W16)=6.07	W27	∑(W27)=5.93
W5	∑(W5)=5.75	W17	∑(W17)=6.08	W28	∑(W28)=6.28
W6	∑(W6)=6.39	W18	∑(W18)=6.10	W29	∑(W29)=5.93
W7	∑(W7)=6.48	O1	∑(O1)=1.68	O2	∑(O2)=1.95
O3	∑(O3)=1.70	O4	∑(O4)=1.91	O5	∑(O5)=2.02
O6	∑(O6)=1.97	O7	∑(O7)=1.69	O8	∑(O8)=1.87
O9	∑(O9)=1.99	O10	∑(O10)=1.36	O11	∑(O11)=1.77
O12	∑(O12)=2.02	O13	∑(O13)=2.14	O14	∑(O14)=1.68
O15	∑(O15)=1.77	O16	∑(O16)=1.98	O17	∑(O17)=1.21
O18	∑(O18)=1.98	O19	∑(O19)=1.64	O20	∑(O20)=1.78
O21	∑(O21)=1.97	O22	∑(O22)=1.86	O23	∑(O23)=1.95
O24	∑(O24)=1.54	O25	∑(O25)=1.78	O26	∑(O26)=1.99
O27	∑(O27)=1.82	O28	∑(O28)=1.93	O29	∑(O29)=1.85
O30	∑(O30)=1.86	O31	∑(O31)=1.03	O32	∑(O32)=1.93
O33	∑(O33)=1.74	O34	∑(O34)=1.81	O35	∑(O35)=1.96
O36	∑(O36)=1.95	O37	∑(O37)=1.83	O38	∑(O38)=1.50
O39	∑(O39)=1.81	O40	∑(O40)=1.79	O41	∑(O41)=1.98
O42	∑(O42)=2.00	O43	∑(O43)=1.59	O44	∑(O44)=1.94
O45	∑(O45)=2.03	O46	∑(O46)=1.97	O47	∑(O47)=1.68
O48	∑(O48)=2.00	O49	∑(O49)=1.96	O50	∑(O50)=1.50
O51	∑(O51)=1.64	O52	∑(O52)=1.78	O53	∑(O53)=1.93
O54	∑(O54)=1.69	O55	∑(O55)=1.80	O56	∑(O56)=2.04
O57	∑(O57)=2.01	O58	∑(O58)=1.69	O59	∑(O59)=2.03
O60	∑(O60)=1.65	O61	∑(O61)=1.91	O62	∑(O62)=1.78
O63	∑(O63)=1.80	O64	∑(O64)=1.89	O65	∑(O65)=1.75
O66	∑(O66)=1.86	O67	∑(O67)=1.59	O68	∑(O68)=2.02
O69	∑(O69)=2.05	O70	∑(O70)=1.83	O71	∑(O71)=2.07
O72	∑(O72)=1.97	O73	∑(O73)=1.64	O74	∑(O74)=1.76
O75	∑(O75)=1.92	O76	∑(O76)=1.99	O77	∑(O77)=1.87
O78	∑(O78)=1.72	O79	∑(O79)=1.75	O80	∑(O80)=2.02
O81	∑(O81)=2.04	O82	∑(O82)=1.63	O83	∑(O83)=2.13
O84	∑(O84)=1.93	O85	∑(O85)=1.82	O86	∑(O86)=1.78

O87	∑(O87)=1.76	O88	∑(O88)=2.00	O89	∑(O89)=1.68
O90	∑(O90)=1.85	O91	∑(O91)=1.93	O92	∑(O92)=1.63
O93	∑(O93)=0.98	O94	∑(O94)=2.02	O95	∑(O95)=1.77
O96	∑(O96)=1.85	O97	∑(O97)=1.75	O98	∑(O98)=1.93
O99	∑(O99)=1.63	O100	∑(O100)=1.68	O101	∑(O101)=1.90
O102	∑(O102)=1.87	O103	∑(O103)=1.63	O104	∑(O104)=1.73
O105	∑(O105)=1.91	O106	∑(O106)=1.59	O107	∑(O107)=1.62

Section4. Selected bond angles and distances of 1

TableS3. Selected representive bond lengths (Å) for 1

Pr(1)-O(1W)	2.649(17)	Pr(2)-O(3W)	2.480(18)	As(1)-O(6)	1.768(18)
Pr(1)-O(105)	2.679(18)	Pr(2)-O(80)	2.53(2)	As(1)-O(18)	1.80(2)
Pr(1)-O(104)	2.672(18)	Pr(2)-O(102)	2.51(2)	As(1)-O(28)	1.80(17)
Pr(1)-O(106)[3]	2.71(2)	Pr(2)-O(4)	2.529(18)	As(2)-O(42)	1.788(17)
Pr(1)-O(107)[3]	2.730(19)	Pr(2)-O(34)	2.499(18)	As(2)-O(53)	1.779(19)
Pr(1)-O(35)	2.401(17)	Pr(2)-O(32)	2.542(19)	As(2)-O(64)	1.810(18)
Pr(1)-O(61)	2.461(18)	Pr(2)-O(70)	2.524(18)	As(3)-O(88)	1.785(19)
Pr(1)-O(69)	2.450(19)	Pr(2)-O(105)	2.541(17)	As(3)-O(98)	1.807(17)
Pr(1)-O(56)	2.503(17)	Pr(2)-N(1)	2.67(2)	As(3)-O(77)	1.872(19)
Pr(1)-O(1W)	2.649(17)	Pr(1)-O(3W)	2.480(18)	N(1)-C(4)	1.32(4)
Pr(1)-O(2W)	2.59(2)	W(20)-O(69)	1.741(19)	N(1)-C(1)	1.28(3)
W(10)-O(35)	1.779(17)	W(20)-O(70)	1.776(18)	N(2)-C(2)	1.27(3)
W(10)-O(34)	1.786(17)	W(20)-O(46)	1.877(17)	N(2)-C(3)	1.29(4)
W(10)-O(31)	1.911(19)	W(20)-O(71)	1.94(2)	O(106)-C(6)	1.27(3)
W(10)-O(36)	1.918(19)	W(20)-O(68)	2.174(17)	O(107)-C(6)	1.26(3)
W(10)-O(37)	2.150(19)	W(20)-O(72)	2.20(2)	N(1)-C(4)	1.32(4)
W(10)-O(24)	2.153(17)				

[3] - X-1,1-Y,-Z

TableS4. Selected representive bond angles (°) for 1

O(6)-As(1)-O(18)	96.2(8)	C(5)-O(104)-Pr(1)	96.0(17)
O(6)-As(1)-O(28)	97.7(8)	C(5)-O(105)-Pr(1)	94.4(16)
O(18)-As(1)-O(28)	97.2(8)	C(5)-O(104)-Pr(2)	96.5(17)
O(42)-As(2)-O(53)	97.0(8)	C(5)-O(105)-Pr(2)	123.3 (17)
O(42)-As(2)-O(64)	96.0(8)	C(6)-O(106)-Pr(1)[3]	93.3(18)
O(53)-As(2)-O(64)	101.3(9)	C(6)-O(107)-Pr(1)[3]	92.8(16)
O(98)-As(3)-O(77)	98.6(8)	W(20)-O(69)-Pr(1)	168.2(10)
O(98)-As(3)-O(98)	97.4(8)	W(20)-O(70)-Pr(2)	141.6(9)
O(88)-As(3)-O(77)	95.6(8)		

[3] - X-1,1-Y,-Z

Section5. The IR spectra

The IR spectrum of **1**, $[As_2W_{19}O_{67}(H_2O)]^{14-}$ precursor and H_2pzdc shows the skeletal vibrations in the range of 2000−450 cm^{-1}. Four characteristic bands appear at 946, 862, 793, and 716 cm^{-1}, which can be assigned to the stretching vibrations ν(W=O), ν(W−O_b−W), ν(As−O_a) and ν(W−O−(As)), respectively.[S1] Three characteristic vibration absorption bonds appear at 1451, 1399 and 1365 cm^{-1} arising from the symmetric and antisymmetric stretching vibration of carboxylate groups, respectively.[S2] The signal at 1625 cm^{-1} is ascribed to the asymmetric stretching vibration $\nu_{as}(COO^-)$, compared with that of pzdc, it displays an obvious slightly red shift, which may be the coordination effect of the rare earth ions and carboxyl (marked with triangle in Figure S3).[S3]

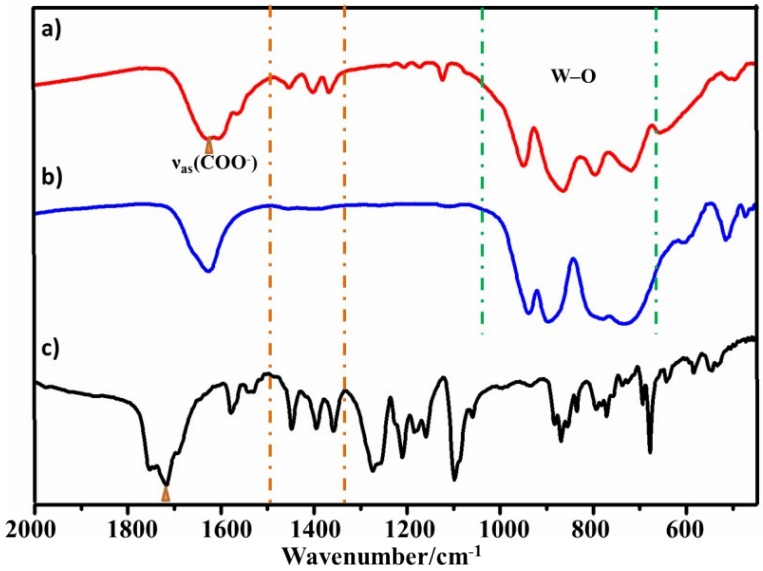

Fig. S3 The IR spectra of **1 (a)** $K_{14}[As_2W_{19}O_{67}(H_2O)]$ (b) and H_2pzdc (c).

Section6. The XPRD patterns

The X-ray powder diffraction experimental pattern of **1** is in good agreement with those of the simulated pattern, indicating the phase purity of the products. The differences in inensity may be due to the preferred orientation of the powder samples during collection of the experimental XRPD pattern.

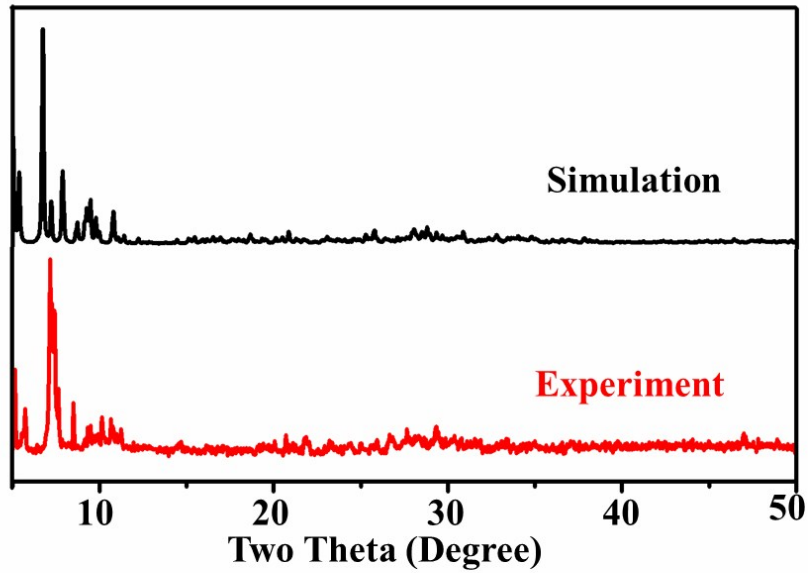

Fig. S4 The XPRD pattern of **1.**

Section7. Thermogravimetric analysis

The thermal behavior of **1** was investigated in a N_2 flow with a heating rate of 10°C·min^{-1} from 25 to 800°C. The TG curve of **1** exhibits two consecutive steps of weight loss. The first step weight losses 4.74% (calcd 4.73%) in the temperature of 25−410 °C, which is assigned to the removal of thirty-eight lattice water molecules and six coordinated water molecules. On further heating, the weight losses between 410−800 °C of 6.95% (calcd 6.53%), arising from the loss of 7.5 structure water, 2 pzdc ligands and the sublimation of 3 As_2O_3 molecules, accompanying with the decomposition of POM skeleton.[S4]

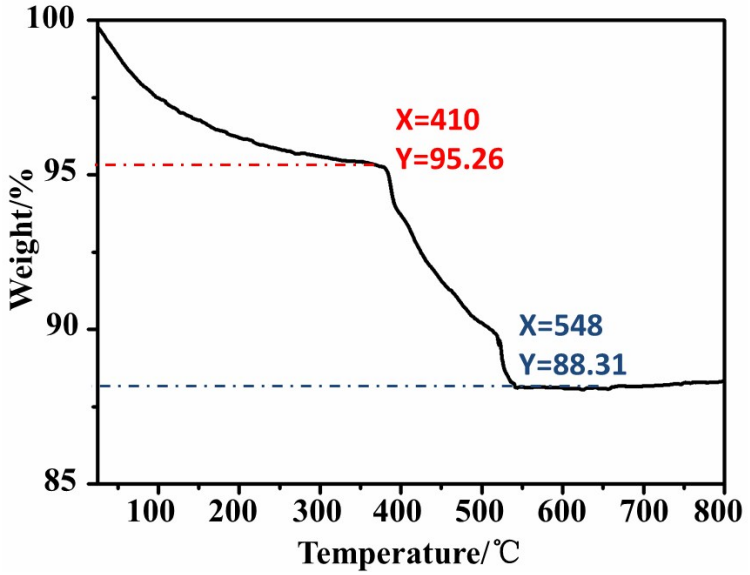

Fig. S5 The thermogravimetric (TG) curve of **1** under N_2 atmosphere.

Section8. Photoluminescence properties

The introduction of RE^{3+} ions into the POM-based clusters may potentially endow these compounds with photoluminescence properties.[S5] Here, the photoluminescence properties and lifetime-decay curves of **1** have been measured at λ_{ex} = 448 nm under ambient temperature. Seven characteristic peaks were observed at λ = 531, 548, 603, 616, 646, 680 and 729 nm, which can be assigned to the $^3P_1 \rightarrow {}^3H_5$, $^3P_0 \rightarrow {}^3H_5$, $^1D_2 \rightarrow {}^3H_4$, $^3P_0 \rightarrow {}^3H_6$, $^3P_0 \rightarrow {}^3F_2$, $^3P_1 \rightarrow {}^3F_2$ and $^3P_0 \rightarrow {}^3F_3$ transitions of the Pr^{3+} ion, respectively.[S6]

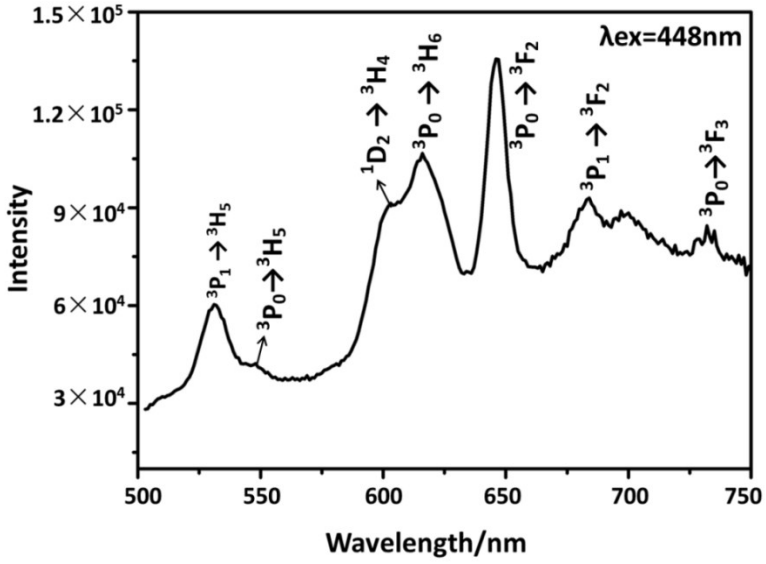

Fig. S6 The luminescence spectrum of **1** under excitation at 448 nm at room temperature.

The decay time profile of **1** was monitored under the most intense emission at λ= 646 nm and excitation at λ = 448 nm. This decay curve can be fitted successfully with a second-order exponential function using the following formula: $I = A_1\exp(t/\tau_1) + A_2\exp(t/\tau_2)$ (where τ_1 and τ_2 are the fast and slow components of the luminescence lifetimes and A_1 and A_2 are the pre-exponential factors). The fitted luminescence lifetimes τ_1 and τ_2 are 0.7 us (50.19%) and 8.1 us (49.81%). Based on the formula $\tau = (A_1\tau_1^2 + A_2\tau_2^2)/(A_1\tau_1 + A_2\tau_2)$,[S7] the average lifetime of **1** can be determined as 4.58 us.

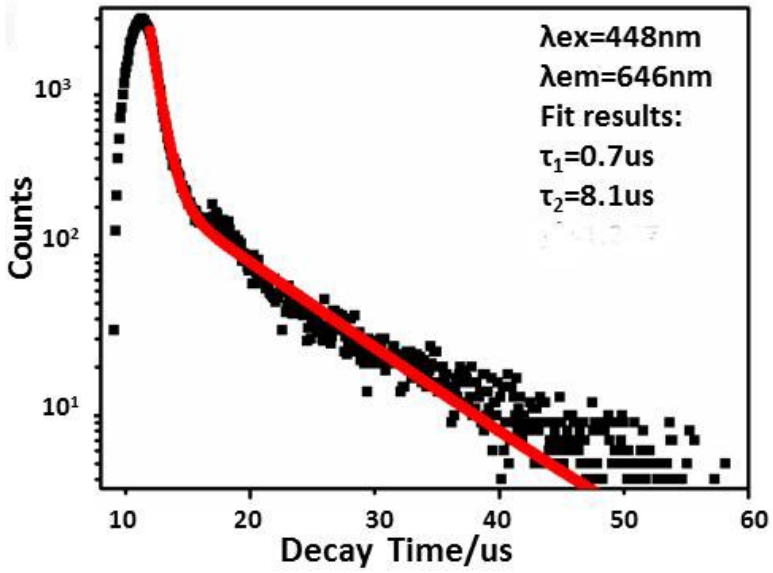

Fig. S7 The decay time curve of **1** under emission at 646 nm at room temperature.

Section9. Catalytic property

Table S5 Epoxidation of cis-cyclooctene with different catalysts[a]

Entry	Catalyst	Con.[b] /%	Sel. / %
1	____	5	99
2	As_2W_{19}	16	98
3	H_2pzdc	4	56
4	$PrCl_3{\cdot}6H_2O$	1	78
5	$PrCl_3{\cdot}6H_2O$+ H_2pzdc	4	64
6	As_2W_{19}+ H_2pzdc	19	96
7	$PrCl_3{\cdot}6H_2O$+ As_2W_{19}	7	93
8	$Na_2[HAsW_9O_{34}]$	11	100
9	$H_6[As_2Mo_{18}O_{62}]{\cdot}28.4H_2O$	8	97
10	Mixture	22	97
11	**Catalyst 1**	**97**	**98**

[a]Reaction conditions: cis-cyclooctene (1 mmol), catalyst (0.05 mol %), n-butyl alcohol (2 mL), 30% H_2O_2 (3 mmol), 65 °C, 4 h; [b] Determined by GC analyses based on the initial substrate.

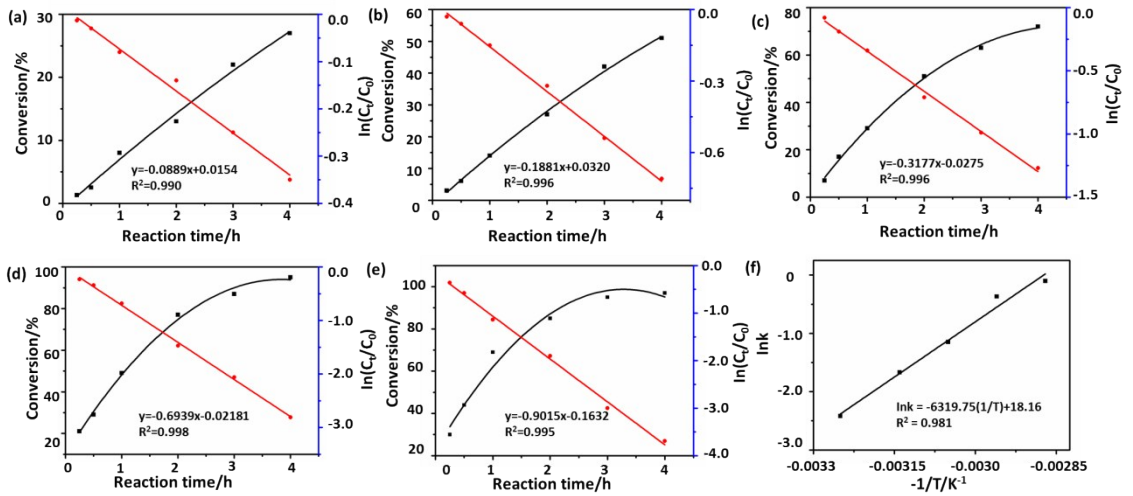

Fig. S8 Kinetic profiles for cis-cyclooctene epoxidation using catalyst **1** at 35 °C (a), 45 °C (b), 55 °C (c), 65 °C (d) and 75 °C (e) in n-butyl alcohol for 4h, respectively. (f) The Arrhenius plot for the cis-cyclooctene epoxidation using catalyst **1** at 35, 45, 55, 65 and 75 °C. The data from different reaction temperatures are fitted to a single straight line, indicating the reaction was pseudo-first-order in cis-cyclooctene (black line: conversion of cis-cyclooctene; red line: $\ln(C_t/C_0)$).

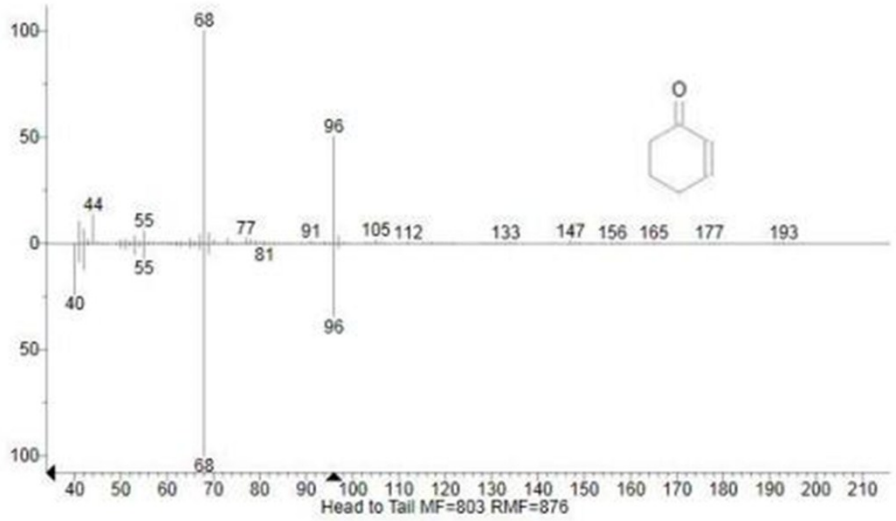

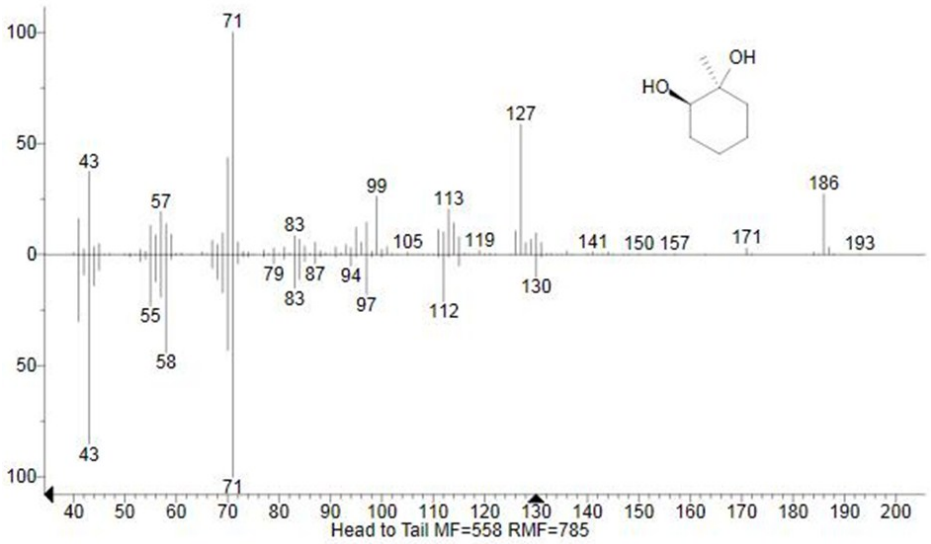

Fig. S9 The mass spectra of the by-products of cyclic olefins (entries 1 and 2 in table 1).

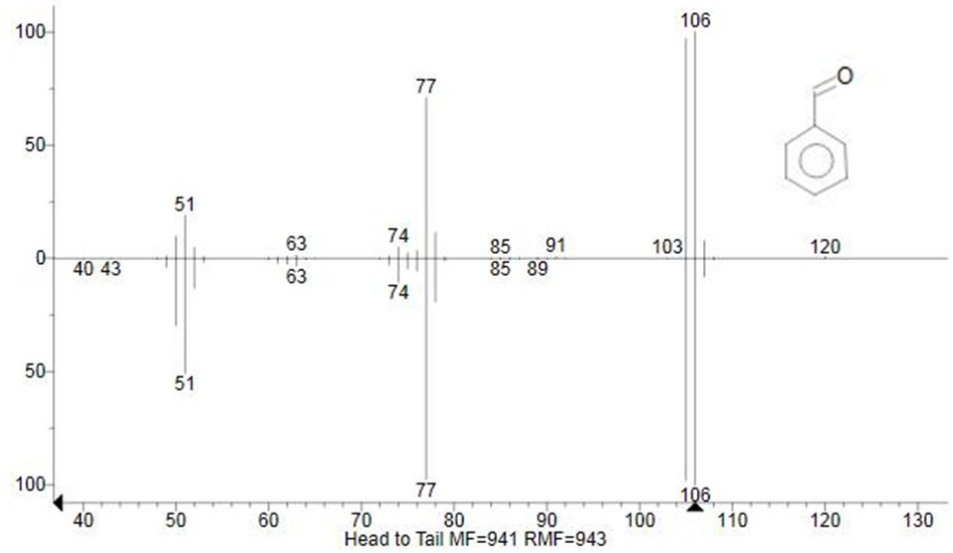

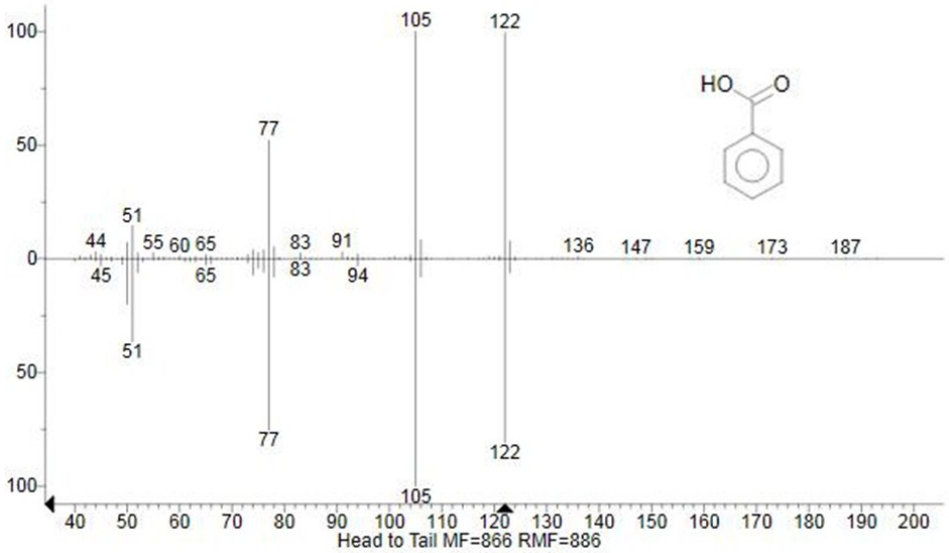

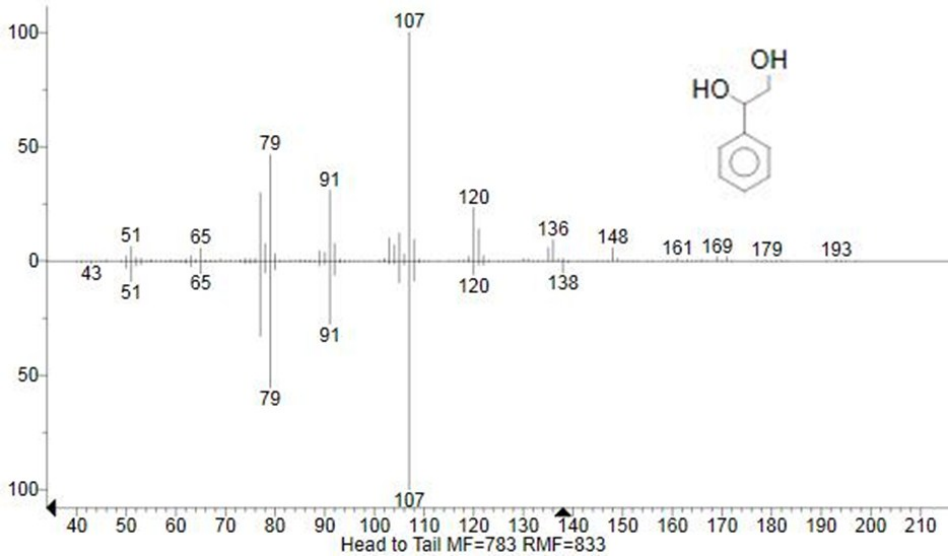
OH
HO
Head to Tail MF=783 RMF=833

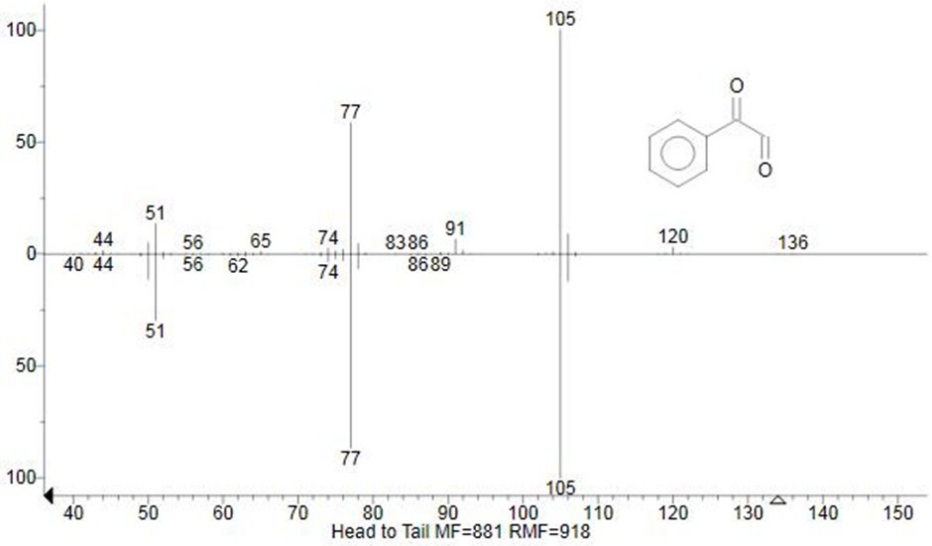
O
O
Head to Tail MF=881 RMF=918

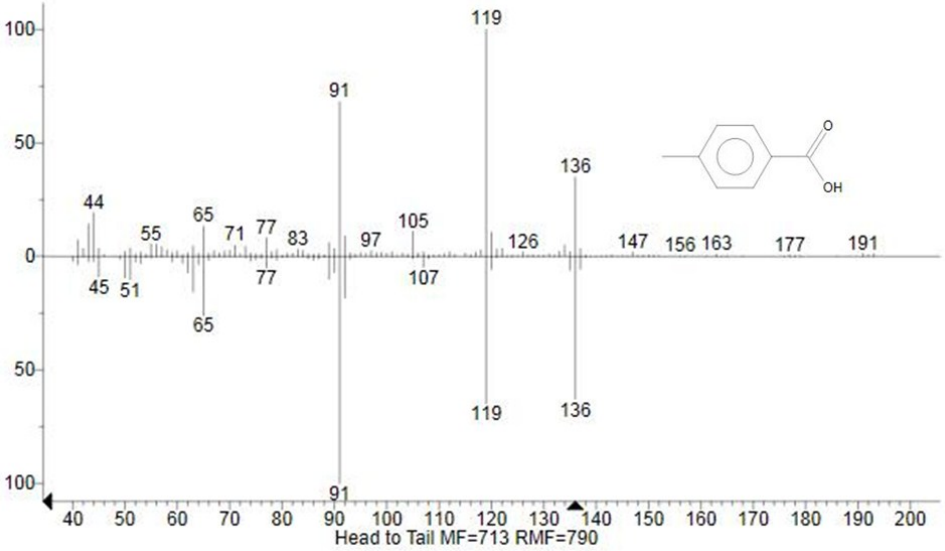
O
OH
Head to Tail MF=713 RMF=790

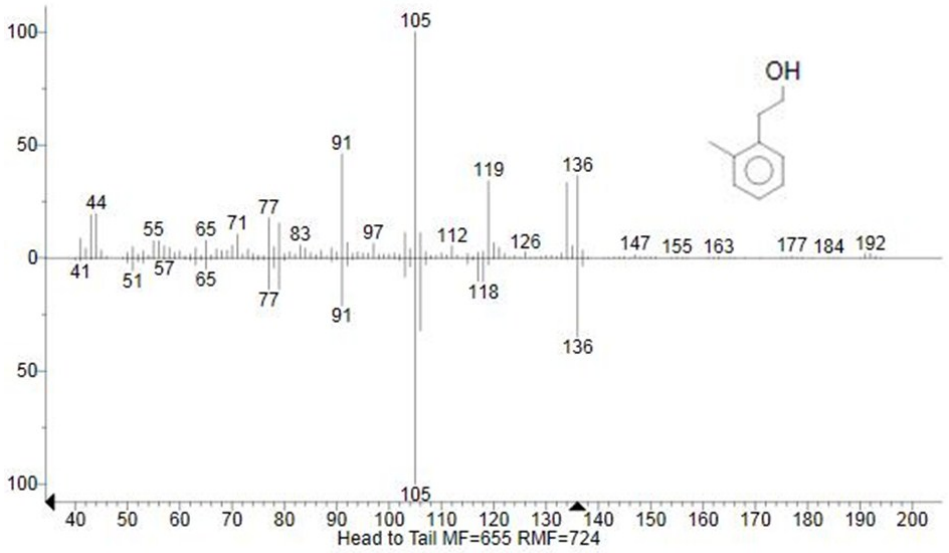

Fig. S10 The mass spectra of the by-products of aromatic olefins (entries 3, 4 and 5 in table 1).

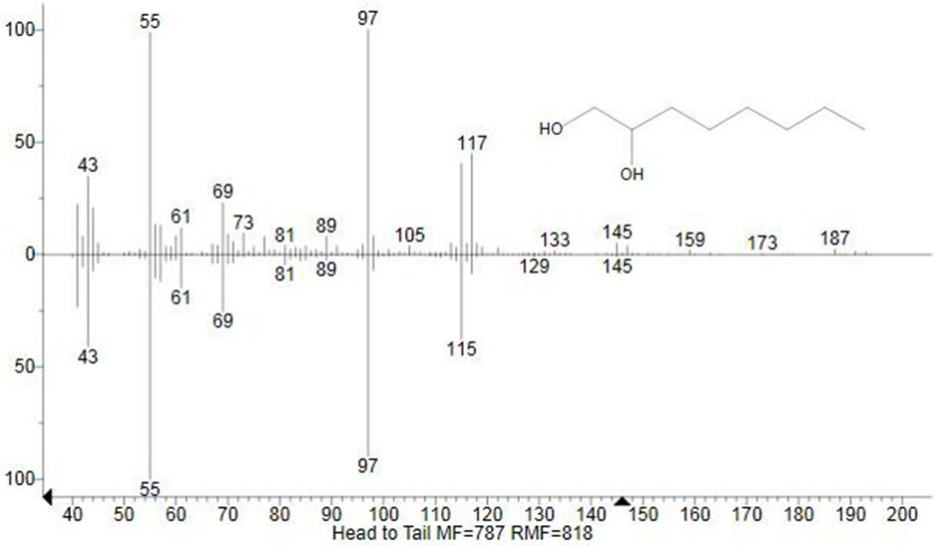

Fig. S11 The mass spectra of the by-products of linear alkenesn (entries 8 in table 1).

Table S6.The comparison of cis-cyclooctene epoxidation activities for various POMs.

Catalyst (catalyst amount)	Reaction conditions	Con./%	TOF/h^{-1} [a]	Ref
$[Fe^{III}_2(NaOH_2)_2(P_2W_{15}O_{56})_2]^{16-}$ (4 mmol)	cis-cyclooctene (1 mmol), CH_3CN (1 mL), 30% H_2O_2(25 μL), T = 25 °C, t = 30 h	98	7.3	S8
$[(Mn^{II}OH_2)_2Mn^{II}_2(As_2W_{15}O_{56})_2]^{16-}$ (0.2 μmol)	cis-cyclooctene (1 mmol), 1,2-dichloroethane (50 mL), 30% H_2O_2(68 μL), T = 25 °C, t = 24 h	n.m.	64.6	S9
$[((MnOH_2)Mn_2PW_9O_{34})_2(PW_6O_{26})]^{17-}$ (2 μmol)	cis-cyclooctene (1 mmol), solvent-free, 30% H_2O_2(68 μL), T = 25 °C, t = 24 h	n.m.	31.5	S10
$[Mn_4(H_2O)_2(PW_9O_{34})]^{10-}$ (4.08 μmol)	cis-cyclooctene (100 mmol), O_2(4 mL/min) and TBHP(0.15 mmol), T = 50 °C, t = 24 h	34	347.2	S11
$DA_{11}[La(PW_{11}O_{39})_2]$ (2.5 μmol)	cis-cyclooctene (1 mmol), CH_3CN (0.2 mL), 30% H_2O_2(1 mmol), T= 25 °C, t = 6 h	98[b]	65.3	S12
$[H_4\{(AsW_9O_{33})Zn(H_2O)W_5O_{11}(N(CH_2PO_3)_3)\}_2(\mu_2\text{-}O)_2]^{10-}$(1 μmol)	cis-cyclooctene (1 mmol), CH_3CN (5 mL), 30% H_2O_2(2 mmol), T = 75°C, t = 8 h	94	116.3	S13
$[\{Pr_3(H_2O)_{10}[Se_2W_{22}O_{76}(gly)_2]\}_2(Se_2W_7O_{30}H_2)]^{18-}$(1 μmol)	cis-cyclooctene (1 mmol), CH_3CN (5 mL), 30% H_2O_2(2 mmol), T = 75°C, t = 6h	94	155	S14
$(Ag_8(mttz)_4(H_2O)[PW^{V}W^{VI}_{11}O_{40}]$ (2.3 mmol)[c]	cis-cyclooctene (7.7 mmol), solvent-free, 30% H_2O_2(10 mmol), T = 70 °C, t = 32 h	70	7.3	S15
$[(CH_3)_4N]_6[Te_2W_{20}O_{70}\{Re(CO)_3\}_2]^{4-}$ (5 μmol)	cis-cyclooctene (1 mmol), CH_3CN (5 mL), 30% H_2O_2(3 mmol), T = 75°C, t = 30 min	98	392	S16
This work	**cis-cyclooctene (1mmol), n-butyl alcohol (2mL), 30% H_2O_2(3mmol), T=65°C, t=4h**	**97**	**485**	

[a] Turnover frequencie (TOF) was calculated by using TOF = conversion of product (mmol)/Catalyst (mmol) x Time (h); [b] Yield; [c] Using a 300 W Xe-lamp to achieve visible-light (>460 nm) irradiation; n.m.: not mentioned.

Table S7 Oxidation of 1-phenylethanol with different catalysts [a]

Entry	Catalyst	Yield [b]
1	——	6
2	$K_{14}[As_2W_{19}O_{67}(H_2O)]$	57
3	H_2pzdc	5
4	$PrCl_3{\cdot}6H_2O$	14
5	$PrCl_3{\cdot}6H_2O$+ H_2pzdc	37
6	As_2W_{19}+ H_2pzdc	78
7	As_2W_{19}+$PrCl_3{\cdot}6H_2O$	61
8	$Na_2[HAsW_9O_{34}]$	56
9	$H_6[As_2Mo_{18}O_{62}]{\cdot}28.4H_2O$	38
10	Mixture	75
11	**Catalyst 1**	**100**

[a] Reaction conditions: 1-phenylethanol (1 mmol), catalyst (0.2 mol%), DMF (3 mL), 30% H_2O_2 (1 mmol), 65 °C, 1 h; [b] Determined by GC analyses based on the initial substrate.

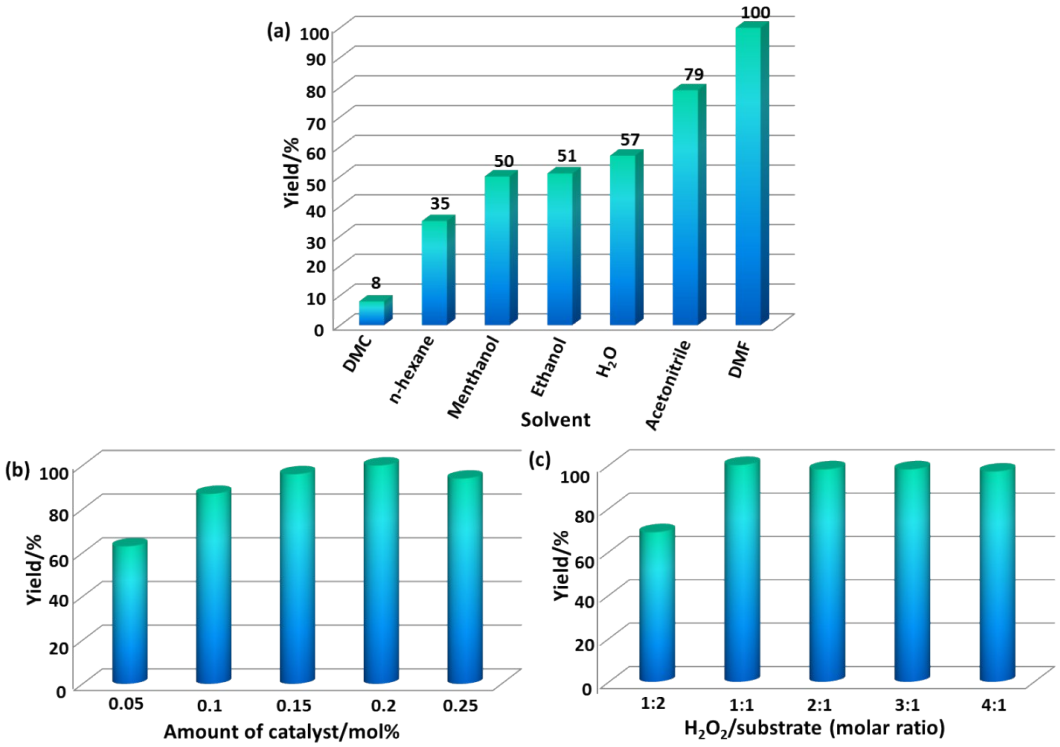

Fig. S12 (a) The oxidation of 1-phenylethanol using different solvents by catalyst **1**. Reaction conditions: 1 mmol 1-phenylethanol, 0.2 mol% catalyst, 1 mmol 30% H_2O_2, T = 65 °C, 1 h; (b) The oxidation of 1-phenylethanol using different amounts of catalyst by catalyst **1**. Reaction conditions: 1 mmol 1-phenylethanol, 3mL DMF, 1 mmol 30% H_2O_2, T = 65 °C, 1 h; (c) The oxidation of 1-phenylethanol using different H_2O_2/substrate molar ratio by catalyst **1**. Reaction conditions: 1 mmol 1-phenylethanol, 0.2 mol% catalyst, 3mL DMF, T = 65 °C, 1 h.

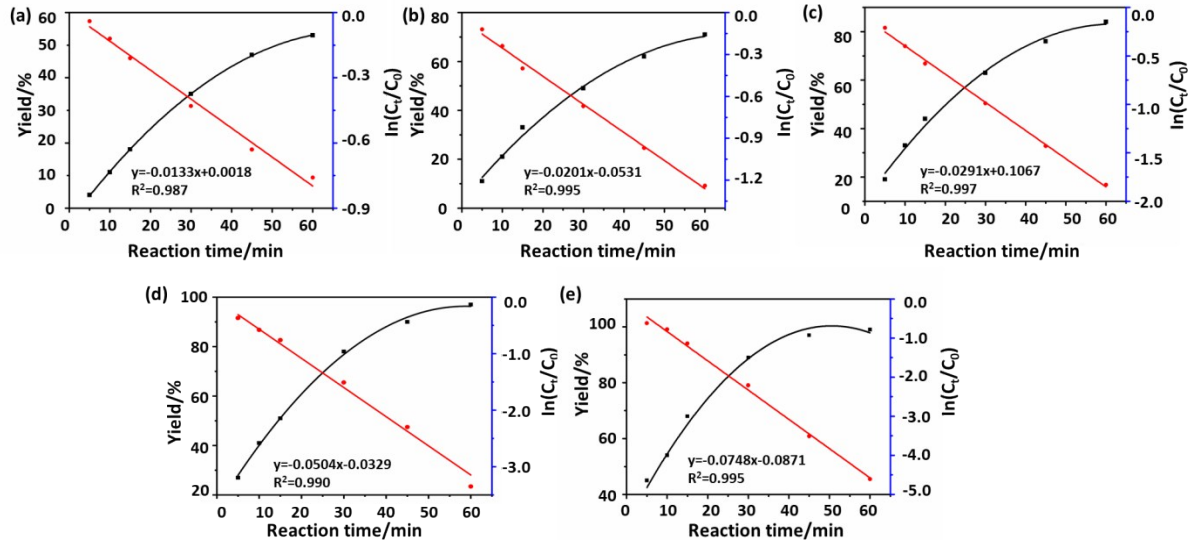

Fig. S13 Kinetic profiles for 1-phenylethanol oxidation using catalyst **1** at 35 °C (a), 45 °C (b), 55 °C (c), 65 °C (d) and 75 °C (e) in 3mL DMF for 1 h, respectively. The data from different reaction temperatures are fitted to a single straight line, indicating the reaction was pseudo-first-order in 1-phenylethanol (black line: yield of 1-phenylethanol; red line: $\ln(C_t/C_0)$).

Table S8.The comparison of 1-phenylethanol oxidation for various POMs.

Catalyst (catalyst amount)	Reaction conditions	Yield/%	TOF[a]	Ref
$[(WZn_3(H_2O)_2][ZnW_9O_{34})_2]^{12-}$ (4 μmol)	1-phenylethanol (1 mmol), H_2O (1 mL), 3% H_2O_2(5 mol), T = 75 °C, t = 7 h	100	35.7	S17
$[SiW_{11}ZnH_2O_{40}]^{6-}$ (2.1 μmol)	1-phenylethanol (1 mmol), H_2O/oil (1 mL), 30% H_2O_2(2 mol), T = 90 °C, t = 7 h	100	68.0	S18
$[\{Zn_2W(O)O_3\}_2H_4\{\alpha\text{-}SiW_9O_{33}\}_2]^{8-}$(4 μmol)	1-phenylethanol (0.5 mmol), acetone (1.5 mL), 30% H_2O_2(0.25 mol), T = 56 °C, t = 1.5 h	92	153.3	S19
$[Zn_4(H_2O)_2(PW_9O_{34})_2]^{10-}$ (9 μmol)	1-phenylethanol (1 mmol), H_2O (3 mL), 30% H_2O_2(5 mol), T = 90°C, t = 3 h	99	36.7	S20
$(V_{14}As_8O_{42}Cl)^{5-}$(2 μmol)	1-phenylethanol (0.1 mmol), Acetone (0.4 mL), 70% TBHP(0.5 mol), T = 25 °C, t = 12 h	100	41.7	S21
$[(Me_2NH_2)Cu(MeCN)V_{12}O_{32}Cl]^{2-}$ (3.3 mmol)	1-phenylethanol (0.33 mol), CH_3CN (1.5 mL), 70% TBHP(0.57 mol), T = 25 °C, t = 6 h	85	14.2	S22
$\{[Ru(phen)_3]_2(V_4O_{12}]\}$(1 μmol)	1-phenylethanol (1 mmol), CH_3CN (3 mL), 70% TBHP(6 mol), T = 60 °C, t = 6 h	97	161.7	S23
$[MoV^{II}{}_4Ru^{IV}{}_2O_{50}(OH)_2]^{10-}$ (1.5 μmol)	1-phenylethanol (1 mmol), CH_3CN (3 mL), 70% TBHP(8 mol), T = 85°C, t = 3 h	100	222.2	S24
$[Cu_5^ICu^{II}(pzc)_2(pz)_{4.5}\{P_2W_{18}O_{62}\}]^-$ (2 μmol)	1-phenylethanol (1 mmol), CH_3CN (1 mL), TBHP (3 mol), T = 60 °C, t = 0.5 h	97	970	S25
This work	**1-phenylethanol (1 mmol), DMF (3 mL), 30% H_2O_2(1 mol), T = 65 °C, t = 1 h**	**100**	**500**	

[a] Turn over frequency (TOF) was calculated by using TOF = conversion of product (mmol)/Catalyst (mmol) x Time (h)

Table S9. Effect of different heteroatoms on catalytic reaction

Entry	Catalyst	Epoxidation of cis-cyclooctene Con.(Sel.) [a]/%	Oxidation of 1-phenylethanol Yield [b] / %
1	$H_3[GeW_{12}O_{40}]$	19 (94)	5
2	$H_3[SiW_{12}O_{40}]$	13 (91)	6
3	$H_3[PW_{12}O_{40}]$	65 (99)	9
4	$H_3[AsW_{12}O_{40}]$	25 (99)	5
5	$K_{14}[P_2W_{19}O_{67}(H_2O)]$	77 (99)	97
6	$K_{14}[As_2W_{19}O_{67}(H_2O)]$	52 (99)	78

[a] Reaction conditions: cis-cyclooctene (1 mmol), catalyst (0.05 mol %), n-butyl alcohol (2 mL), 30% H_2O_2 (3 mmol), 100 °C, 4 h; [b] Reaction conditions: 1-phenylethanol (1 mmol), catalyst (0.2 mol %), DMF (3 mL), 30% H_2O_2 (1mmol), 100 °C, 1 h.

References

S1. W. L. Chen, Y. G. Li, Y. H. Wang, E. B. Wang, Z. M. Su, *Dalton Trans.,* 2007, 4293–4301.
S2. U. Kortz, M. G. Savelieff, B. S. Bassil and M. H. Dickman, *Angew. Chem., Int. Ed.,* 2001, **40**, 3384–3386.
S3. Nakamoto, K. Infrared and Raman Spectra of Inorganic and Coordination Compounds, Part B, 6th ed.; Wiley: New York, 2009.
S4. J. Niu, K. Wang, H. Chen, J. Zhao, P. Ma, J. Wang, M. Li, Y. Bai and D. Dang, *Crystal Growth Design,* 2009, **9**, 4362–4372.
S5. H.-L. Cui, S.-Z. Zhan, M. Li, S. W. Ng, D. Li, *Dalton Trans.,* 2011, **40**, 6490–6493.
S6. L.-L. Li, R. Pan, J.-W. Zhao, B.-F. Yang, G.-Y. Yang, *Dalton Trans.,* 2016, **45**, 11628-11632.
S7. T. Fujii, K. Kodaira, O. Kawauchi, N. Tanaka, H. Yamashita and M. Anpo, *J. Phys. Chem., B,* 1997, **101**, 10631–10637.
S8. Zhang, X.; Anderson; T. M.; Chen, Q.; Hill, C. L. *Inorg. Chem.,* 2001, **40**, 418–419.
S9. I. M. Mbomekalle, B. Keita, L. Nadjo, P. Berthet, W. A. Neiwert, C. L. Hill M. D. Ritorto and T. M. Anderson, *Dalton Trans.,* 2003, 2646–2650.
S10. M. D. Ritorto, T. M. Anderson, W. A. Neiwert and C. L. Hill, *Inorg Chem.,* 2004, **43**, 44–49.
S11. K. Patel, B. K. Tripuramallu and A. Patel, *Eur. J. Inorg. Chem.,* 2011, **2011**, 1871–1875.
S12. S. Zhao, Y. Jia and Y.-F. Song, *Appl. Catal., A: G.,* 2013, **453**, 188–194.
S13. Huo, Y.; Huo, Z. Y.; Ma, P. T.; Wang, J. P.; Niu, J. Y.; *Inorg. Chem.,* 2015, **54**, 406–408.
S14. L. Yang, L. Li, J. Guo, Q. Liu, P. Ma, J. Niu and J. Wang, *Chem - Asian J.,* 2017, **12**, 2441–2446.
S15. X. Lin, M. Zhang, M. Zhu, H. Huang, C. Shi, Y. Liu and Z. Kang, *Inorg. Chem. Front.,* 2018, **5**, 2493–2500.
S16. J. Lu, X. Ma, P. Wang, J. Feng, P. Ma, J. Niu and J. Wang, *Dalton Trans.,* 2019, **48**, 628–634.
S17. D. Sloboda-Rozner, P. Witte, P. L. Alsters and R. Neumann, *Adv. Synth. Catal.,* 2004, **346**, 339–345.
S18. J. Wang, L. Yan, G. Li, X. Wang, Y. Dingand J. Suo, *Tetrahedron Lett.,* 2005, **46**, 7023–7027.
S19. Y. Kikukawa, K. Yamaguchi and N. Mizuno, *Inorg. Chem.,* 2010, 49, 8194–8196.
S20. Y. Ding, W. Zhao, B. Ma and W. Y. Qiu, Can. *J. Chem.,* 2011, 89, 13–18.
S21. M. L. Campbell, D. Sulejmanovic, J. B. Schiller, E. M. Turner, S.-J. Hwu and D. C. Whitehead, *Catal Sci. Technol.,* 2016, **6**, 3208–3213.
S22. K. Kastner, M. Lechner, S. Weber and C. Streb, *Chemistry Select*, 2017, **2**, 5542–5544.
S23. K. Wang, Q. Xu, P. Ma, C. Zhang, J. Wang and J. Niu, *CrystEngComm*, 2018, **20**, 6273–6279.
S24. R. Wan, Q. Xu, Mengdan Han, P. Ma, C. Zhang, J. Niu and J. Wang, *Materials*, 2018, **11**, 178.
S25. D. Li, Q. Xu, Y. Li, Y. Qiu, P. Ma, J. Niu and J. Wang, *Inorg. Chem.*, 2019, **58**, 4945–4953.